

Polymeric Nanoreactors for Hydrophilic Reagents Synthesized by Interfacial Polycondensation on Miniemulsion Droplets

Daniel Crespy, Michael Stark, Carola Hoffmann-Richter, Ulrich Ziener, and Katharina Landfester*

Department of Organic Chemistry III—Macromolecular Chemistry and Organic Materials, University of Ulm, Albert-Einstein-Allee 11, 89081 Ulm, Germany

Received September 21, 2006; Revised Manuscript Received February 6, 2007

ABSTRACT: We describe a versatile method to obtain functional hollow nanoreactors with a hydrophilic liquid core. The synthesis of hollow polyurea, polythiourea, and polyurethane nanocapsules was performed by interfacial polycondensation or cross-linking reactions in inverse miniemulsion. The miniemulsions were built upon emulsification of a solution of amines or alcohols in a polar solvent with cyclohexane as the nonpolar continuous phase. The addition of suitable hydrophobic diisocyanate or diisothiocyanate monomers to the continuous phase allows the polycondensation or the cross-linking reactions to occur at the interface of the droplets. The wall thickness of the capsules can be directly tuned by the quantity of the reactants. The nature of the monomers and the continuous phase are the critical factors for the formation of the hollow capsules, which is explained by the interfacial properties of the system. The resulting polymer nanocapsules could be subsequently dispersed in water. The capsules were found to be spherical when formamide was used as the liquid core, whereas elongated capsules were obtained with water. Finally, we used these hollow nanoreactors as a model system for the preparation of silver nanoparticles by reducing silver nitrate solutions encapsulated by the polyurea shell. These syntheses are the first that allow the encapsulation of hydrophilic compounds in miniemulsion in a hollow structure.

Introduction

The synthesis of hollow polymeric capsules with sizes ranging from 50 nm to 50 μm has an intense interest in materials science. They offer unique properties as nano- or microreactors and are suitable materials for drug delivery systems. There are generally two approaches to make hollow polymeric particles, which can be differentiated by the presence or absence of a sacrificial core. In the first method, a core particle is used as template and therefore coated with a polymeric shell. The coating of the sacrificial core is obtained by adsorption of a preformed polymer or by polymerization on the surface of the core; subsequently, the core is removed by chemical or physical means as dissolution or calcination. The technique of formation of a polymeric shell by adsorption on a sacrificial core comprises the layer-by-layer technique, putting alternatively polyelectrolytes or nanoparticles of opposite charges on a mineral or organic sacrificial core. This method was used for capsule diameters ranging from 70 nm to 10 μm . The thickness of the capsule wall is simply controlled by the number of cycles of the layer-by-layer deposition.^{1–5} Hollow spheres of 200–400 nm were also obtained by dissolution or enzymatic degradation of the core of noncovalently connected core–shell micelles.⁶ Fleming et al. synthesized hollow microcapsules via assembly of polystyrene nanoparticles (100–200 nm) on silica microparticles (3–10 μm), followed by heating the polymer above T_g to give a homogeneous shell and finally chemical etching of the silica with HF.⁷ The assembly proceeded via chemical (amine–aldehyde) or biochemical (avidin–biotin) interactions between the nanoparticles and the microparticles. The polymer shell can also be created by polymerization around the sacrificial core. Thus, polymeric shells were polymerized in a dispersion process.^{8–12} Living polymerizations (ATRP and anionic polymerization) confined at the surface of a silica core with

potential subsequent etching of this core can lead to hollow polymeric capsules, too.^{13–18} Marinakos et al. obtained hollow nanocapsules via the polymerization of pyrrole and *N*-methylpyrrole on gold nanoparticles followed by etching of the gold particles (50–300 nm).¹⁹ The thickness of the nanocapsules was controlled by the polymerization time. Finally, an original lost-wax technique was reported to synthesize nanoparticles and nanocapsules in an inverse opal.²⁰

Obviously, the techniques that do not use a sacrificial core are more suitable since they need less steps for the synthesis. In this case, the shell formation is driven by self-assembly or by surface tension forces. Thus, capsules can be made by the “ouzo effect”,²¹ the self-assembly of block copolymers,²² the photopolymerization of a monomer in phospholipid liposomes,²³ cross-linking of polymerizable liposomes,²⁴ or neutralization of a polymeric charged core.²⁵ Hollow particles were successfully obtained by phase separation during a suspension ($\sim 5 \mu\text{m}$)²⁶ or an emulsion polymerization²⁷ process (0.2–1 μm). A particular seeded emulsion polymerization with the dynamic swelling technique gave hollow capsules because of the self-assembling of phase-separated polymer (SaPSeP) at the interface with the aqueous medium ($\sim 2 \mu\text{m}$).²⁸ The same method allows the preparation of cured epoxy micron-sized hollow particles.²⁹ The well-known interfacial polycondensation technique can be applied also to dispersed systems. Thus, the microemulsion process was used for the microencapsulation of osmium tetroxide,³⁰ palladium(II) acetate, and Pd(0) (20–250 μm) in a polyurea matrix.³¹ The polyurea was synthesized by polycondensation at the interface of the oil droplets. However, the synthesis did not lead to hollow capsules, but rather to solid core particles.

Recently, the miniemulsion technique was found to be a suitable technique for the synthesis of well-defined nanocapsules because of the high stability of the droplets. Such stability ensures a copy 1:1 from the droplets to the final object (nanoparticle or nanocapsule). It was also found possible to

*Corresponding author: Fax (+49) 7315022883; e-mail katharina.landfester@uni-ulm.de.

Table 1. Typical Composition of the Miniemulsions for the Synthesis of Nanoparticles and Nanocapsules

composition		polyurea nanocapsules	polyurethane nanocapsules	polythiourea nanocapsules
dispersed phase	polar solvent [g]	1.3	1.3	1.3
	monomer 1 or polymer: hydrophilic [g]	0.1	0.1	0.1
	lipophobe NaCl [g] or lipophobe AgNO ₃ [g]	0.03	0.03	0.03
		0.02–0.12		
continuous phase	apolar solvent [g]	7.5	7.5	7.5
	surfactant P(B/E- <i>b</i> -EO) [g]	0.075	0.075	0.075
second part of continuous phase	apolar solvent [g]	5	5	5
	surfactant P(B/E- <i>b</i> -EO) [g]	0.035	0.035	0.035
	monomer 2: hydrophobic [g]	0.25	0.28	0.30

create nanocapsules with an aqueous core with the direct use of a polymer instead of polymerizing monomers. Thus, our group reported on the synthesis of poly(methyl methacrylate) capsules by controlled nanoprecipitation of the polymer on stable droplets of an inverse miniemulsion.³² Several groups have reported that hydrophobic compounds could be efficiently encapsulated in thin shells made by free-radical polymerization.^{33–35} Torini et al. have described the encapsulation of hydrophobic compounds by interfacial polycondensation in miniemulsion.³⁶ The process took place in a direct system (o/w) where the stable diisocyanate IPDI was reacted with the 1,6-hexanediol monomer at the interface of the droplets. The capsule morphology was not evidently shown. Scott et al. described an original synthesis of nanocapsules in direct miniemulsion via interfacial free-radical polymerization.³⁷ A surface active initiator was used to start an alternating copolymerization between one monomer present in the dispersed oil phase and a monomer present in the aqueous continuous phase. Breitenkamp and Emrick developed a method for the synthesis of larger capsules (~40 μm) made by cross-metathesis at the oil in water droplets interface.³⁸ Additionally, a completely different approach was recently reported by Im et al.³⁹ First, polystyrene nanospheres were swollen with toluene to increase their volumes followed by freezing with liquid nitrogen. The freezing involves shrinkage of the particles and hence the creation of a void inside the particles due to the liquid to solid phase transition of toluene. The toluene is then evaporated below 0 °C, leaving a hole at the particle surface because of the flux of toluene. The final materials are hollow polystyrene nanocapsules.

Up to now, there is only one report in the interfacial polycondensation in a miniemulsion system. Taira et al. recently described the trap and release of oligo-nucleotide using pH-responsive amphoteric particles.⁴⁰ We present the synthesis of hollow nanocapsules with an aqueous core and a shell made of polyurea, polythiourea, or polyurethane as obtained in an inverse miniemulsion process. These nanoreactors are used for the reduction of silver nitrate to silver nanoparticles as model reactions. This is to our knowledge the first time that inorganic nanoparticles suspended in an hydrophilic phase are encapsulated in a hollow structure without the use of a sacrificial core.

Experimental Part

Chemicals. The hydrophilic monomers 1,4-diaminobutane (DAB), 1,6-diaminohexane (HMDA), diethylenetriamine (DET), glycerol, 1,6-hexanediol (all 99%), and 3,4-diaminobenzoic acid (DBA, 97%) were purchased from Aldrich. L-Arginine (Ph Eur, USP) was purchased from Merck-Schuchardt. The hydrophilic polymers dextran from *Leuconostoc* spp. ($M_r \sim 70\,000\text{ g mol}^{-1}$) and soluble starch from potatoes ($M_r = 162.14\text{ g mol}^{-1}$) were purchased from Fluka. Water-free high molecular weight poly(ethylene imine) (PEI) was purchased from Aldrich. Toluene, 2,4-diisocyanate (TDI, 98%) and hexamethylene diisocyanate (HMDI, 98%) were purchased from Fluka while isophorone diisocyanate (IPDI, 98%) and tolylene

2,4-diisothiocyanate (TDIT, 97%) were purchased from Aldrich. The salts sodium chloride, sodium hydroxide, and silver nitrate were p.a. chemicals from Merck. Formamide (99.5%) from Aldrich and demineralized water were used throughout the work. The reducing agent hydrazinium hydroxide (99%) was purchased from Merck. All these reagents were used as received. *N*-Vinylformamide (*N*-VFA, 98%) and 1-vinyl-2-pyrrolidone (1-V2P, 99%+), both from Aldrich, were distilled under reduced pressure. Dimethyl sulfoxide (DMSO) from Merck and 2-pyrrolidone from Aldrich (99%+) were dried under CaH₂ for 15 h and then distilled under reduced pressure. Hydrazine (98%) was purchased from Aldrich and potassium persulfate (99%) from Fluka. The block copolymer emulsifier poly[(butylene-*co*-ethylene)-*b*-(ethylene oxide)], P(B/E-*b*-EO), consisting of a poly(butylene-*co*-ethylene) block ($M_w = 3700\text{ g mol}^{-1}$) and a poly(ethylene oxide) block ($M_w = 3600\text{ g mol}^{-1}$) was synthesized by anionic polymerization.⁴¹ Cyclohexane was refluxed with CaH₂ for 15 h and then distilled from the CaH₂.

Synthesis of Hollow Nanocapsules. A typical procedure occurred in the following way: 0.1 g of the amino-monomer or hydroxyl-containing monomer or hydrophilic polymer (monomer 1), 1.3 g of the polar solvent in the droplets that form the liquid core, and 30 mg of NaCl were mixed at room temperature. This mixture was then added to a solution of a specific amount of the P(B/E-*b*-EO) surfactant in 7.5 g of the continuous phase (cyclohexane was used as nonpolar phase if not otherwise mentioned). After stirring 1 h with a magnetic stirrer for pre-emulsification, the miniemulsion was prepared by ultrasonication of the mixture for 180 s at 70% amplitude (Branson sonifier W450 Digital, tip size 6.5 mm) with ice cooling in order to prevent polymerization. Then a defined amount of diisocyanate or diisothiocyanate (monomer 2) dissolved in cyclohexane with 35 mg of P(B/E-*b*-EO) was added to the miniemulsion usually for 300 s, if not otherwise mentioned. The mixture was allowed to react for 2 h at 25 °C for the polyurea nanocapsules, and at 60 °C for the polyurethane, the cross-linking of starch or dextran, and the formation of the polythiourea nanocapsules. For the radical polymerization of 1-vinyl-2-pyrrolidone inside the nanoreactors, a controlled amount of this monomer and the initiator potassium persulfate (KPS) was added to the dispersed phase. For the reduction of silver nitrate in the nanocapsules, a specific amount of silver nitrate was added to the dispersed phase and acted as the lipophobe instead of the sodium chloride. Two different methods were chosen for the reduction of the silver ions: (i) 0.2 mL of hydrazinium hydroxide was added to the miniemulsion, or (ii) a macroemulsion containing 0.2 mL of hydrazinium hydroxide, 2 mL of cyclohexane, and 0.1 g of P(B/E-*b*-EO) was added to the miniemulsion. For both methods, the miniemulsion was ultrasonicated during the addition for 60 s with pulses of 5 s and pauses of 3 s at 70% amplitude (Branson sonifier W450 Digital, tip size 6.5 mm) with ice cooling and was kept overnight at 25 °C. Typical formulations of the latexes are shown in Table 1, and the overall synthesis of the capsules loaded with silver nanoparticles is schematically summarized in Figure 1. The dispersion of the nanocapsules in water was obtained via the following way: 0.15 g of the synthesized latex dispersion was mixed with a solution of 5 mg of SDS in 6 g of water. The resulting mixture was ultrasonicated for 1 min at 70% amplitude (Branson sonifier W450 Digital, tip size 6.5 mm) with ice cooling. Then the

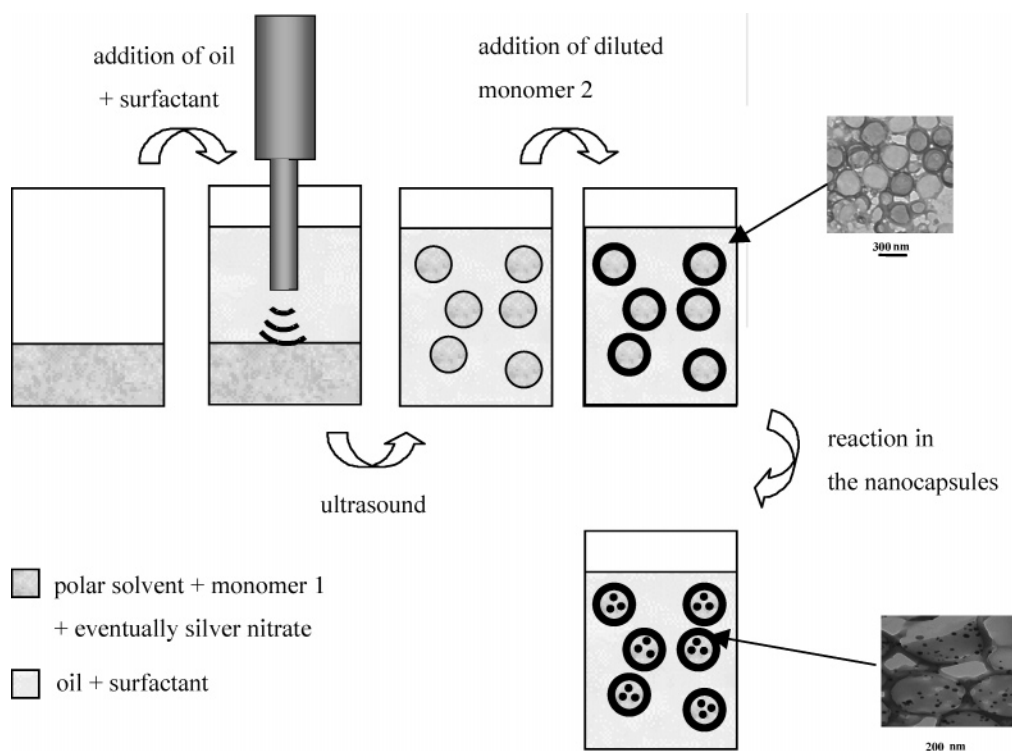


Figure 1. Synthesis of polymeric capsules with eventual use as nanoreactors for the reduction of silver nitrate.

weight of the dispersion was reduced by 10% by evaporation of the continuous phase and the cyclohexane and subsequently put in an ultrasonic bath for 5 min. This procedure was found to be more suitable than the traditional freeze-drying technique in order to redispersed the nanocapsules. In the case of completely dried nanocapsules, the nanocapsules stuck irreversibly together.

Analytical Methods. The particle sizes were measured by photocorrelation spectroscopy using a Nicomp particle sizer (model 370, PSS Santa Barbara, CA) at a fixed scattering angle of 90° . The data were processed using the cumulants method. Further laser light scattering experiments were performed with an ALV-Instruments ALV/CGS-8F laser goniometer system and ALV-5000 multi- τ digital correlator to determine the R_g/R_h ratio of the nanocapsules. The light source was a JDS Uniphase helium/neon 22 mW laser operating at $\lambda = 633$ nm. The correlation functions obtained were analyzed using the CONTIN program, and the scattering angle was varied from 20° to 150° . Electron microscopy was performed with a Phillips 400T TEM operating at 80 kV. The miniemulsions were diluted in cyclohexane and then applied to a 400 mesh carbon-coated copper grid and left to dry. No further contrasting was applied. Scanning electron microscopy (SEM) micrographs were obtained with a DSM 962 SEM (Zeiss, Germany). Gravimetric measurements were performed with a Kern RH 120-3 gravimeter to measure the solid content of the latexes. The FT-IR measurements were performed to check the structure of the polymer with KBr pellets in a FTIR 113v Bruker spectrophotometer equipped with a DTGS detector using 100 signal-averaged scans at a resolution of 2 cm^{-1} . The solid used for the IR measurements was obtained by drying the miniemulsion for 96 h at 40°C under vacuum, then washing the solid with water and hexane, and drying the solid again. UV-vis analyses were carried out with a Perkin-Elmer UV-vis spectrometer Lambda 16. The latexes were 50 times diluted (w/w) in dried cyclohexane. Calorimetry was performed with a Micro Reaction calorimeter μ -RC from THT. Samples of 0.5 mL of the miniemulsion were prepared, and 280 μL of the diiso-(thio)cyanate in cyclohexane and surfactant was subsequently added to study the kinetics of the reaction at 20°C for the polyurea shell and at 60°C for the polythiourea and the polyurethane shells. Reference experiments without diiso(thio)cyanate were performed to determine the contribution of the energy of mixing of the liquid added to the miniemulsion to the evolution of heat. Atomic force

microscopy was performed during evaporation of the cyclohexane continuous phase with a soft cantilever in the contact mode (MFP-3D microscope, Asylum Research), after evaporation of the cyclohexane, after drying the latex deposited on the substrate in a desiccator for 12 h, and after submitting the latex deposited on the substrate to high vacuum for 10 min (all tapping mode). The sample was prepared either by dropping or by spin-coating a 10 wt % diluted latex on mica substrates.

Results and Discussion

Nanocapsules were synthesized according to the procedure shown in Figure 1. A solution of the first monomer in a hydrophilic solvent is miniemulsified by ultrasonication in a solution of surfactant in a hydrophobic solvent. The first monomer is then located in the droplets. A solution of the second monomer in the hydrophobic solvent is then added to the miniemulsion. The polymer is formed by polycondensation of the hydrophilic and the hydrophobic monomers. This should lead to the formation of capsules; however, in some cases it does not, as will be discussed below. Additionally, it is possible to dissolve silver nitrate in the hydrophilic solvent prior to the miniemulsification. Miniemulsion droplets containing silver nitrate and the first monomer are then formed. The second monomer is subsequently added to the miniemulsion, leading to the formation of a polymer followed by the introduction of a reducing agent, which reduces the silver nitrate to silver nanoparticles in the miniemulsion droplets.

As shown in Table 2, it was possible to synthesize either polyurea nanoparticles or nanocapsules in inverse miniemulsion, depending on the reagents used, but at fixed wt % ratios of monomers compared to the dispersed phase. The P(B/E-*b*-EO) surfactant was found to stabilize efficiently the capsules in inverse miniemulsion against coalescence, while a little amount of NaCl was used as lipophobe since it is known to stabilize inverse miniemulsion latexes against Ostwald ripening when water is the dispersed phase.⁴² As shown in Table 2, we performed experiments with different dispersed phases: DMSO (entries P1–P4), 1-vinyl-2-pyrrolidone (entries P5–P6), *N*-

Table 2. Characteristics of the Miniemulsions That Give Either Nanoparticles or Nanocapsules^a

entry	dispersed phase		continuous phase		object ^b	polymer	diam ^c (nm)
	solvent	monomer 1	solvent	monomer 2			
P1	DMSO	HMDA	cyclohexane	HMDI	P	polyurea	190
P2	DMSO	DET	cyclohexane	HMDI	P	polyurea	213
P3	DMSO	DET	cyclohexane	IPDI	P	polyurea	242
P4	DMSO	DET	cyclohexane	TDI	P	polyurea	100
P5	1-V-2-P	DET	cyclohexane	HMDI	P, U	polyurea	130
P6	1-V-2-P	DET	cyclohexane	TDI	P, U	polyurea	109
P7	N-VFA	DET	cyclohexane	HMDI	P	polyurea	178
P8	N-VFA	DET	cyclohexane	TDI	P	polyurea	154
P9	2-pyrrolidone	DET	cyclohexane	HMDI	P, U	polyurea	181
P10	2-pyrrolidone	DET	cyclohexane	TDI	P, U	polyurea	165
P11	formamide	DET	cyclohexane	HMDI	P	polyurea	191
P12	formamide	DET	cyclohexane	IPDI	P	polyurea	272
P13	formamide	DET	cyclohexane	TDI	C	polyurea	250
P14	formamide	DET	toluene	TDI	C + P	polyurea	265
P15	formamide	DET	hexane	TDI	C	polyurea	292
P16	formamide	DET	cyclohexane	bisphenol A diglycidyl ether	P	epoxy resin	250
P17	formamide	DET	cyclohexane	TDIT	C	polythiurea	377
P18	formamide	HMDA	cyclohexane	TDI	C	polyurea	175
P19	formamide	cysteamine: 10 wt % DET: 90 wt %	cyclohexane	TDIT	C	polythiurea polyurea	424
P20	formamide	glycerol	cyclohexane	TDI	C	PU	203
P21	formamide	1,6-hexanediol	cyclohexane	TDI	U	PU	n.m.
P22	formamide	DBA	cyclohexane	TDI	C	polyurea	281
P23	formamide	PEI	cyclohexane	TDI	C	cross-linked PEI	571
P24	formamide	starch	cyclohexane	TDI	C	cross-linked starch	497
P25	water	DET	cyclohexane	HMDI	C	polyurea	329
P26	water	DET	cyclohexane	TDI	C	polyurea	216
P27	water	DAB	cyclohexane	TDI	C	polyurea	354
P28	water	HMDA	cyclohexane	TDI	C	polyurea	381
P29	water	1,6-hexanediol	cyclohexane	TDI	U	PU	n.m.
P30	water	L-arginine	cyclohexane	TDI	C	polyurea	378
P31	water	starch	cyclohexane	TDI	C	cross-linked starch	524
P32	water	dextran	cyclohexane	TDI	C	cross-linked dextran	324

^a The weight ratios monomer/polar solvent/surfactant/continuous phase are kept constant. ^b P = particles, C = capsules, U = unstable. ^c Determined by DLS.

vinylformamide (entries P7–P8), 2-pyrrolidone (entries P9–P10), formamide (entries P11–P24), and water (entries P25–32) were used as liquid cores. We could synthesize either particles or capsules depending on the nature of these liquid cores.

Synthesis of the Nanoparticles. Miniemulsion polycondensation was carried out by the reaction between a monomer dissolved in a polar solvent that builds the droplets and a second monomer, which comes from the continuous phase, i.e., from outside the droplets. The results summarized in Table 2 show that when DMSO (P1–P4), 1-vinyl-2-pyrrolidone (P5–P6), *N*-vinylformamide (P7–P8), or 2-pyrrolidone (P9–P10) was the polar solvent in the dispersed phase, polyurea nanoparticles and no nanocapsules were formed independently from the monomers that were employed (see morphologies in Figure 2). With DMSO as the polar solvent, the combinations of monomers HMDA/HMDI (P1), DET/HMDI (P2), DET/IPDI (P3), and DET/TDI (P4) were used. With 1-vinyl-2-pyrrolidone as the polar solvent, the combinations of monomers DET/HMDI (P5) and DET/TDI (P6) were carried out. The combinations of monomers DET/HMDI (P7) and DET/TDI (P8) were tried with *N*-VFA as the polar solvent. And finally, the combinations DET/HMDI (P9) and DET/TDI (P10) were also performed with 2-pyrrolidone as the polar solvent.

In the case of 1-vinyl-2-pyrrolidone as polar solvent, it can function additionally as monomer, which can be polymerized via free-radical polymerization. Thus, we performed a miniemulsion polycondensation as described above with 1-vinyl-2-pyrrolidone as the dispersed phase and then polymerized the 1-vinyl-2-pyrrolidone. Remarkably, the nanoparticles were

crumpled when only 1-vinyl-2-pyrrolidone was used as both polar solvent and monomer for free-radical polymerization (without formamide or water), as shown in Figure 3. In our case, the reaction is performed in an inverse system, and hence the use of TDI yielded stable particles. Takasu and Kawaguchi also reported the formation of spherical polyurea shell/polystyrene core particles but in a direct miniemulsion.⁴³ In their case, the TDI monomer was found not to be suitable in such case to obtain stable latexes because of its high reactivity. The reactivity is then lowered compared to the reactivity observed with the less reactive IPDI monomer. In our case, the reaction is performed in an inverse system, and hence the use of TDI yielded stable particles.

The DMSO and the 1-vinyl-2-pyrrolidone are obviously not hydrophilic enough, and therefore the hydrophilicity differences are not significant enough to create the nanocapsule structure. So, the nanocapsule formation is not the thermodynamic favorite structure, and solid particles are formed instead.

Synthesis of Nanocapsules. It is suitable to provide heterophase synthesis that allows the formation of nanomaterials other than plain particles. In fact, the nanocapsule morphology is particularly interesting due to the capacity of the shell to encapsulate a large amount of material in the core. In the following we have investigated the influence of the composition of the dispersed phase on the latex morphology.

Polyurea Capsules. Water and formamide are more hydrophilic and were found to be more suitable for the formation of nanocapsules than the other polar solvents described above, i.e., DMSO, 1-vinyl-2-pyrrolidone, *N*-VFA, and 2-pyrrolidone. The successful synthesis of nanocapsules was also closely related

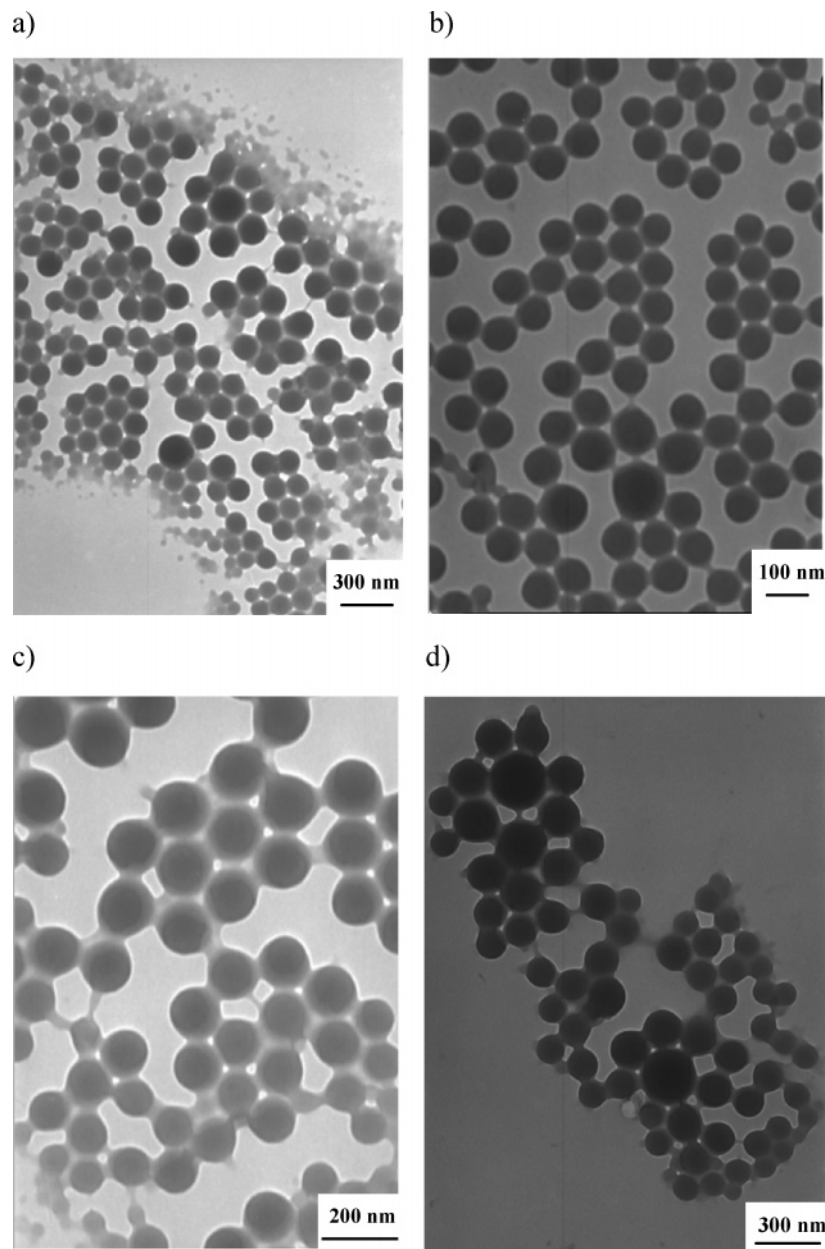


Figure 2. TEM micrographs of polyurea particles. Samples P3 (DET and IPDI as monomers), P5 (DET and HMDI as monomers), P7 (DET and HMDI as monomers), and P9 (DET and HMDI as monomers).

to the kind of monomers for water and formamide as liquid core. Thus, the reaction between tolylene 2,4-diisocyanate and either diethylenetriamine, 1,6-diaminohexane, or 1,4-diaminobutane yields a nanocapsule morphology when water is the liquid core, as shown in Table 2 (entries P26–P28). With water, the reaction between diethylenetriamine and hexamethylene diisocyanate gave also nanocapsules (entry P25). When formamide is the liquid core, the reaction between tolylene 2,4-diisocyanate and diethylenetriamine or hexamethylenediamine formed nanocapsules (entries P13 and P18, respectively). The reaction between diethylenetriamine and the diisothiocyanate was found to be suitable to form a nanocapsule morphology (entry P17), too, whereas the reaction of diethylenetriamine with hexamethylene diisocyanate (entry P11) or IPDI (entry P12) or bisphenol diglycidyl ether (60 °C to form epoxy resin, entry P16) yielded nanoparticles. With formamide as liquid core, the use of hexane instead of cyclohexane for the continuous phase gives also nanocapsules (entry P15), whereas toluene as continuous phase gives a mixture of nanoparticles and nano-

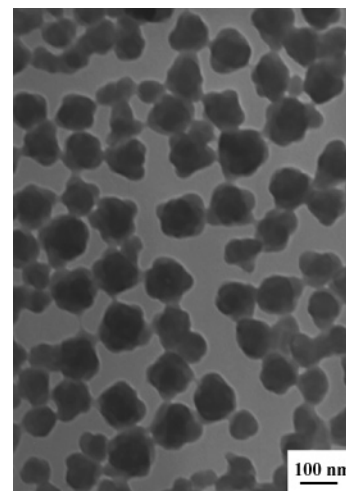


Figure 3. TEM micrographs of the poly(vinylpyrrolidone)/polyurea (DET and TDI as monomers) hybrid nanoparticles (entry P6).

Table 3. Dependence of the Size of the Particles on the Dispersed Phase, on the Time of Addition of the Diisocyanate Solution, and on the Concentration of Surfactant

entry	dispersed phase	time of addition of the solution of hydrophobic monomer (s)	surfactant (wt %)	diameter in cyclohexane (nm) ^a	diameter in water (nm) ^a
variation of the amount of surfactant					
P33	formamide	300	2.3	1212	unstable
P34	formamide	300	4.4	258	766
P13	formamide	300	6.5	250	584
P35	formamide	300	8.6	160	228
P36	formamide	300	13	153	378
variation of the time of addition					
P37	formamide	600	6.5	275	591
P38	formamide	1200	6.5	331	385
P26	water	300	6.5	216	414
P39	water	600	6.5	235	227
P40	water	960	6.5	260	293

^a Determined by DLS.

capsules (~70% of nanoparticles and ~30% of nanocapsules according to the TEM measurements, entry P14). All these results can be interpreted in term of phase separation and interfacial tension. A suitable system for the formation of nanocapsules is obtained when the hydrophilic monomer and the hydrophobic monomer tends to form a polymer, which will phase-separate at the interface of the droplets. This means that despite the principle of the synthesis of the nanoparticles and the nanocapsules is the same, i.e., one monomer in the droplets and one monomer outside the droplets, different morphologies of the latex are obtained depending on the composition of the dispersed phase.

Polyurea nanocapsules with functional carboxylic acid groups could be synthesized with 3,4-diaminobenzoic acid (entry P22) with formamide as liquid core, or L-arginine (entry P30) with water as liquid core, as hydrophilic monomers. They could hence eventually be used as pH-responsive nanocontainers.⁴⁰ The reaction with amino acids is of special interest for the use in biomedical application. The principle of the synthesis described above was extended to the cross-linking of functional polymers. The process allows one also to use poly(ethylene imine), starch, or dextran as hydrophilic monomers. Here, an interfacial cross-linking of poly(ethylene imine) (P23), starch (P24, P31), and dextran (P32) with TDI gave also nanocapsule morphologies.

Table 3 shows that the size of the polyurea capsules with formamide or water as liquid cores is influenced by the amount of surfactant as expected for the miniemulsion technique (entries P33–P36); i.e., the particle size decreases when the concentration of surfactant increases.⁴⁴ A nanocapsule size of 258 nm could be reached with 4.4 wt % surfactant compared to the dispersed phase (entry P34). By using 8.6 wt % surfactant compared to the dispersed phase (entry P35), we could even obtain a nanocapsule size down to 160 nm. This is approximately the minimum size attainable since the use of more surfactant did not significantly change the nanocapsule diameter. Our synthesis involves the addition of the second monomer to miniemulsion droplets containing the first monomer. The addition time of the second monomer may have an influence on the colloidal properties of the latex. Thus, we analyzed the influence of the addition time of the second monomer to the miniemulsion on the capsule size. Nanocapsules with different times of addition of the solution of tolylene 2,4-diisocyanate were prepared (entries P13, P37–P38 with formamide as liquid core and P26, P39, P40 with water as liquid core). As shown in Table 3, the addition time of the solution of diisocyanate monomer to the miniemulsion plays an important role for the size of the nanocapsules. With increasing addition time from 300 to 1200 s, the nanocapsules size also increases from 250 to 331 nm with

formamide as the liquid core and from 216 to 260 nm with water as the liquid core. A control experiment was made without the addition of the diisocyanate monomer and presents droplets with a hydrodynamic diameter of 235 nm, close to the value of the experiment with fast addition (sample P13: 250 nm). Therefore, a fast addition “freezes” the original state of the droplets by forming a solid polymer shell. Conversely, a slower addition may allow some rearrangements in the polymer conformation of the polymer building the shell, thus leading to larger hydrodynamic diameter of the capsule compared to the diameter observed with a fast addition. The fact that the hydrodynamic diameter of the capsule is smaller in the case of a fast than for a slow addition may be due to the hindrance of the Ostwald ripening by the rapid formation of a solid polymer shell.

In fact, calorimetric measurements shown in Figure 4 reveal that the polymerization is very fast. The samples with a short addition time of 300 s (P13 with a formamide core, P26 with an aqueous core) have a reaction time of about 500 s and display a single heat peak. The samples with a longer addition time of 600 s (P37 with a formamide core, P39 with an aqueous core) display several heat peaks, which correspond to the different injections of the second monomer. They have a reaction time of about 600 s. Finally, the reaction profile of the polythiourea formation is a single peak with a reaction time of about 700 s. This means that the reaction is very fast and that the time of reaction is almost the time of addition of the second monomer.

Variation of the Wall Thickness. We showed that it is possible to synthesize nanocapsules via interfacial polycondensation in inverse miniemulsion. We could vary the size of the capsules simply by changing the amount of surfactant in the formulation. It would be also interesting to vary the wall thickness of the nanocapsules, which would probably be a key parameter in the control of the release behavior of these nanocontainers. Because the monomers are the building material of the capsule wall, we studied the influence of the amount of monomer on the wall thickness of the capsules. It is expected that the larger the amount of monomers is, the thicker the wall of the capsules should be. The results shown in Table 4 indicate that the amount of hydrophilic monomer has an influence on the wall thickness of the nanocapsules. Conversely, the variation of the amount of hydrophilic (e.g., DET) or hydrophobic monomers (e.g., TDI) has no significant influence on the diameter of the nanocapsules. Table 4 shows that the concentration of the diethylenetriamine monomer in the droplets is the critical factor for the control over the wall thickness. In fact, for different amounts of diethylenetriamine, the wall thickness is significantly varied from 15 nm for entry P45 to 39 nm for

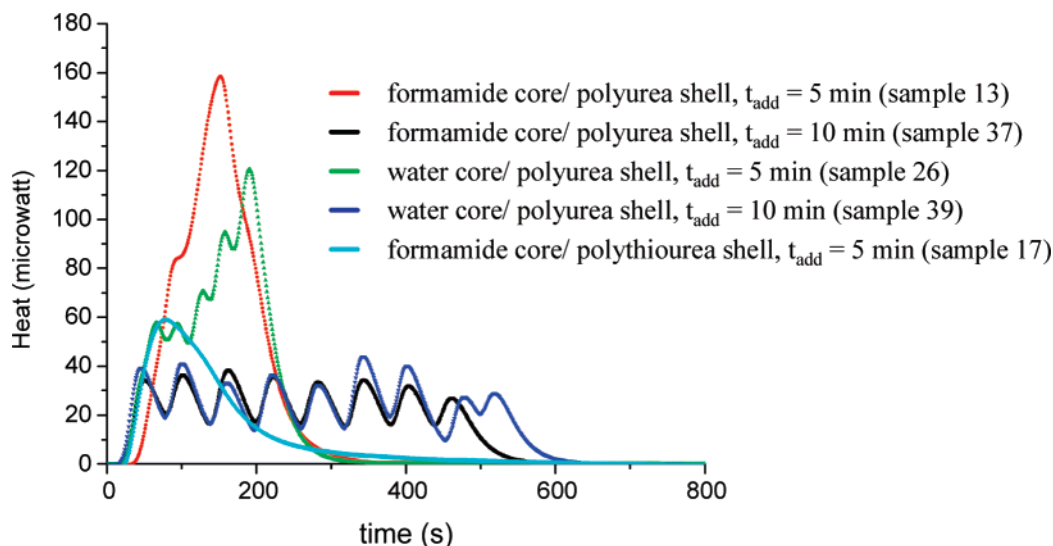


Figure 4. Calorimetry curves of the reaction performed with different time of addition of the second monomer (t_{add}). The different peaks are the consequence of the noncontinuous (discrete) nature of the addition.

Table 4. Characteristics of the Polyurea Latexes with Formamide as Liquid Core Synthesized with Different Amounts of Monomers

entry	DET (g)	TDI (g)	diameter (nm) ^a	diameter in water (nm) ^a	diameter (nm) ^b	wall thickness (nm) ^b
P41	0.2	0.5	272	625	221	39
P13	0.1	0.26	250	584	209	23
P42	0.1	0.13	218	833	192	24
P43	0.1	0.05	213	807	203	20
P44	0.055	0.13	244	381	189	15
P45	0.05	0.06	202	546	196	13

^a Determined by DLS. ^b Determined by TEM.

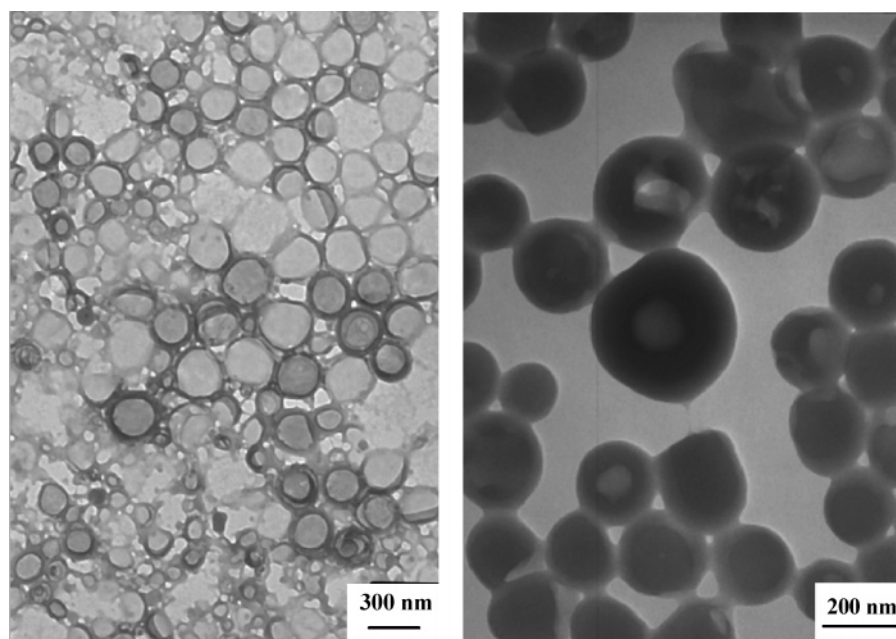


Figure 5. TEM micrographs of polyurea nanocapsules prepared with different amount of monomers: (a) entry P13; (b) entry P41 prepared with a double amount of monomers compared to entry P13.

entry P41. The wall thickness can be then controlled simply by varying the amount of monomer in the formulation, as shown in Figure 5. It is observed that the wall thickness is much larger if the mass of monomer is increased in the miniemulsion formulation and that the nanocapsules still keep a spherical shape independently on the amount of monomers employed. The amount of diisocyanate does not play a significant role for the wall thickness: entries P13, P42, P43 and entries P44 and P45 have the same wall thickness. In fact, the loss of volume due to the use of less diisocyanate is compensated by the fact that

the less cross-linked polyurea has more freedom to expand.

Morphology of the Capsules. As shown in Figure 6, the synthesized nanocapsules have a hollow structure detected by TEM with a thin polymeric wall. The nanocapsules with formamide as liquid core are spherical whereas some of the nanocapsules with water as the liquid core have a prolate spheroid shape (olive-shaped). As shown in Figure 7, sample P26 with an aqueous core is composed of big nonspherical capsules and small spherical nanocapsules. The particles produced in heterophase polymerization processes are most often

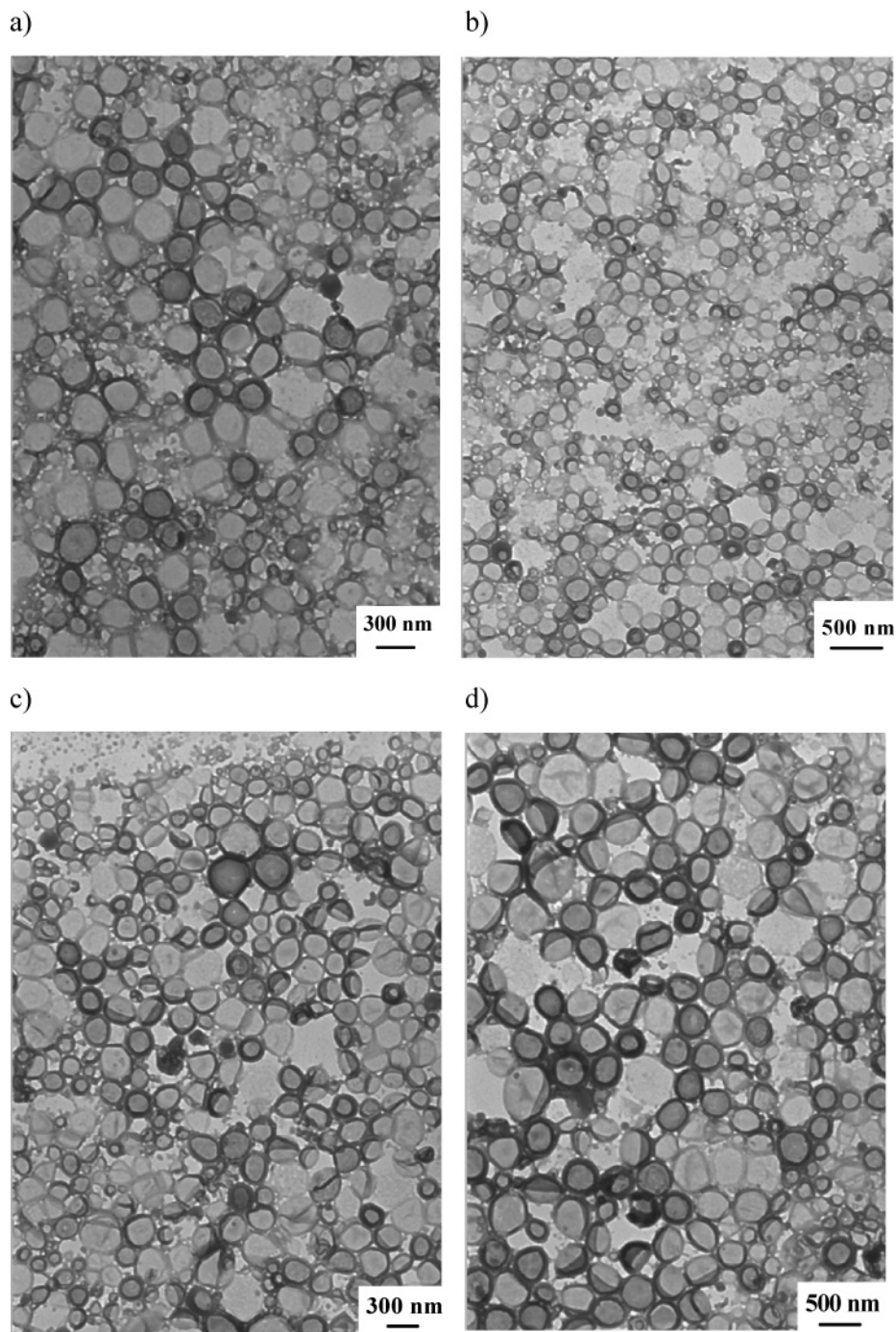


Figure 6. TEM micrographs of the samples P13 (a, b) and P37 (c, d) prepared with formamide as the liquid core. The capsules have a spherical shape.

spherical since the system tends to minimize the interfacial energy between the two phases. One exception was reported in the case of miniemulsion polymerization of ϵ -caprolactam.⁴⁵ Ellipsoidal particles of polyamide-6 were formed because of the phase separation that occurred in the miniemulsion droplets between the polyamide and the DMSO. Xu et al. reported that thin polymeric capsules can be irreversibly deformed during the process by the evaporation of the liquid core even for highly cross-linked capsules because they are more flexible than thick capsules.¹² In our case, the nanocapsules formed with water are more deformable than those with formamide as dispersed phase. Indeed, some of the isocyanate groups reacted with the water as revealed by the presence of urea groups in IR spectra, hence increasing the brittleness of the polymer.

We investigated further the structure of the polyurea nanocapsules with water as liquid core by AFM measurements because in the wet state they should not be deformed by any external forces. The measurements were taken in the presence of the cyclohexane as continuous phase, or after evaporation at room temperature, or after letting the deposited latex in a desiccator for 12 h, or finally submitting the deposited latex to vacuum for 10 min. The images shown in Figure 8 indicate that only some of the large capsules are deformed while the nanocapsules stayed intact. This observation confirms the TEM data, i.e., the presence of some large deformed capsules in coexistence with spherical nanocapsules. Therefore, it can be concluded that the large capsules are originally in dispersion spherical and become crumpled when they are submitted to a

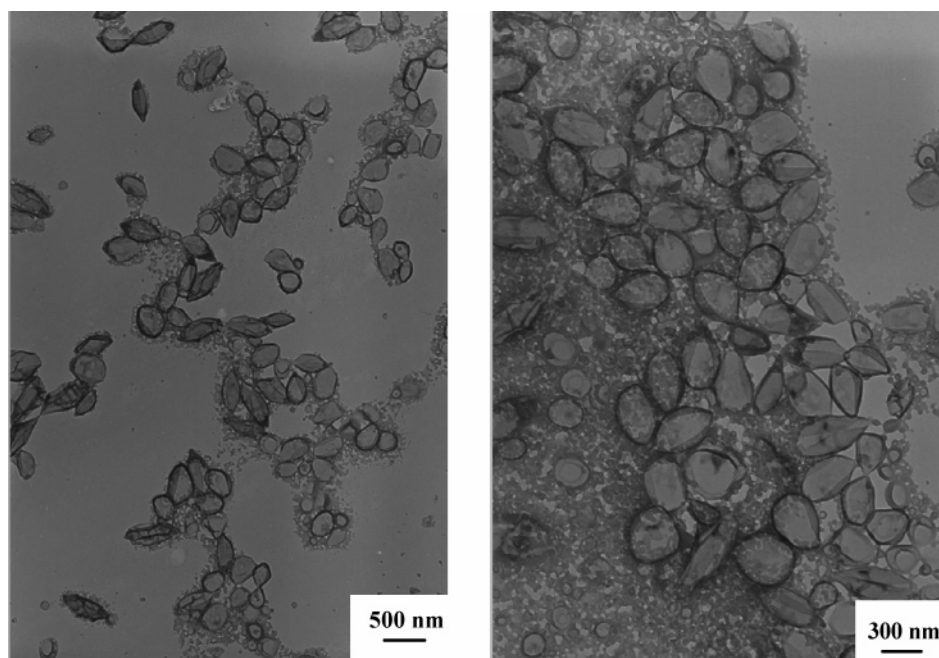


Figure 7. TEM micrographs of the sample P26 prepared with an aqueous core. The capsules have a prolate spheroid shape.

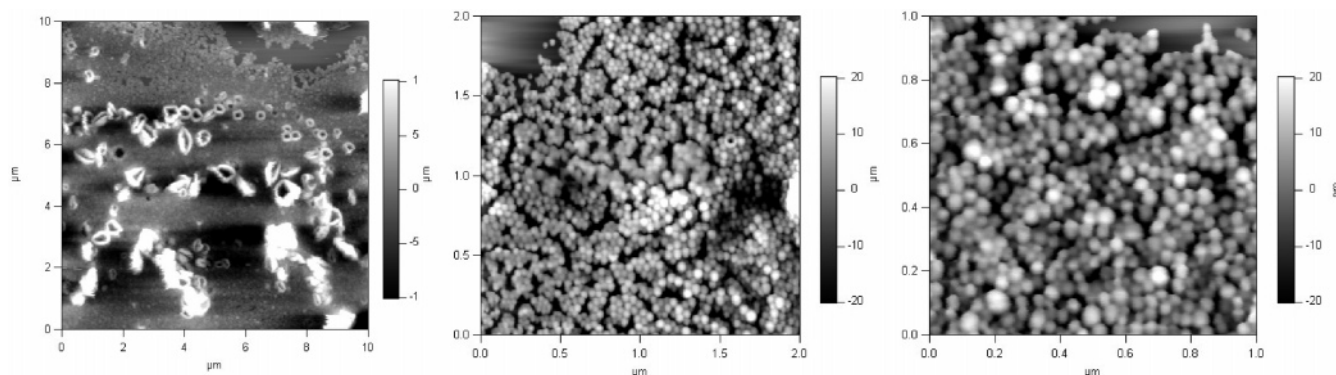


Figure 8. AFM micrographs of sample P26.

certain force. In fact, according to Yang et al., the deformation of the nanocapsule-like objects could be explained by effect of the force of the AFM cantilever.⁴⁶ Besides, SLS combined with DLS measurements show that the capsules with water do not have the typical scattering behavior of an ellipsoid but rather the one of a sphere (see Figure 9). SLS measurements can provide information about not only the size and the molecular weight but also the shape of an object by analyzing the scattering behavior of this object at different angles and concentrations. However, the capsules with water as liquid core did not show the deviation at higher scattering angles expected for an ellipsoidal shape. This observation indicates that the nanocapsules have a spherical shape in the wet state.

The capsules made of cross-linked starch displayed also some other interesting morphologies, as shown in Figure 10. When water was the liquid core, the capsules have spherical morphologies (sample P31). When formamide is the liquid core (sample P24), the capsules collapsed in the TEM due to the strong vacuum. The mechanical properties of starch seem to be different in the presence of water or formamide, which would explain the observed differences in morphologies.

Dispersion in Water. Up to now the capsules are dispersed in an organic solvent. A transfer to an aqueous dispersion would be suitable for eventual biomedical applications. The dispersion of nanocapsules in cyclohexane was taken and mixed with an

aqueous solution of SDS. The mixture was treated in a sonication bath and then ultrasonicated for a short time. The cyclohexane was then evaporated. This procedure was chosen in order to achieve a minimum size of the droplets of cyclohexane in the system. In fact, with such conditions, we can assume that the system is composed of droplets of cyclohexane with a minimum of nanocapsules per droplet down to one nanocapsule per droplet and empty cyclohexane droplets. If the size of the cyclohexane droplets would be bigger, the redispersion being provided by a standard stirring system, they would contain several nanocapsules. During the subsequent evaporation process of the cyclohexane, the droplets of cyclohexane shrink and would lead to coalescence of the nanocapsules. The procedure described in the Experimental Part is also preferable to the traditional freeze-drying technique since the nanocapsules tend to stick together upon removing of the continuous phase. The dispersion in water is accompanied by an increase of the hydrodynamic diameter, depending on the quality (nature) of the dispersed phase (see Table 4). The use of formamide as dispersed phase instead of water prevents subsequent hydrolysis of still nonreacted isocyanate groups. Hence, the capsules containing formamide are submitted to hydrolysis to amino groups during the dispersion in water. These groups are highly hydrophilic and drive the capsules toward an expansion in water.

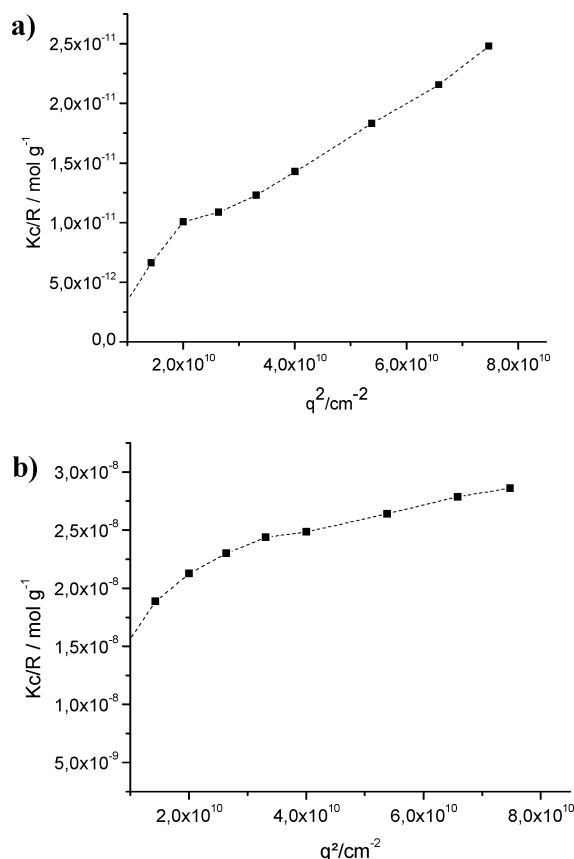


Figure 9. SLS measurements of the latexes: (a) sample P13 with a formamide core; (b) sample P26 with an aqueous core.

Polythiourea and Polyurethane Capsules. Polythiourea capsules containing formamide in the core were successfully obtained with the process discussed before for polyurea capsules (see Table 2). For the synthesis of polythiourea capsules, the tolylene 2,4-diisocyanate used for the formation of polyurea capsules was replaced by an equivalent molar amount of tolylene 2,4-diisothiocyanate (P17, P19); the choice of the amine is quite flexible. Similarly, polyurethane capsules were synthesized at 60 °C by using an equivalent molar amount glycerol instead of the diethylenetriamine monomer in the dispersed phase (P20). After the removal of the surfactant and the continuous phase, the polymers were identified by IR as polythiourea and

polyurethane, respectively, free from urea groups. The IR spectra of polythiourea capsules showed characteristic bands at 3430, 3199, 1528, and 1265 cm^{-1} , whereas polyurethane capsules exhibited corresponding bands at 1720, 1540, and 1220 cm^{-1} . Remarkably, the polyurethane capsules formed monolayers while packing upon deposition of the miniemulsion on TEM grids, as shown in Figure 11. Additionally, it was shown by DLS measurements that the speed of cooling of the latexes has no influence on their stability.

Polyurea Nanocapsules as Nanoreactors. Because of their hollow structure, the nanocapsules can be used as nanocontainers for reactions in hydrophilic media. We chose the reduction of silver nitrate in silver nanoparticles as model system to show that the polyurea capsules can be used as nanoreactors. The preparation of the silver nanoparticles loaded capsules involves the dissolution of silver nitrate in the dispersed phase followed by the polymerization of the shell. The metal salt is subsequently reduced by the addition of hydrazine to the miniemulsion under short ultrasonication, which diffuses through the thin capsule wall. Ultrasonication is used to facilitate the migration of the hydrazine through the cyclohexane to the capsules since the hydrazine is not soluble in the cyclohexane continuous phase. To check the reactivity of hydrazine toward our dispersed phase, nonencapsulated droplets containing silver nitrate were reduced in a control experiment. Figure 12 shows the silver nanoparticles obtained via this process. We investigated then the formation of polyurea capsules followed by the reduction of the encapsulated silver nitrate by hydrazine. It was possible to prepare capsules loaded with different amounts of silver inside as shown in Table 5, simply by varying the concentration of the silver salt in the dispersed phase from 1.2 to 6.8 wt % with respect to the dispersed phase. We chose hydrazine as reducing agent to guarantee a fast reducing process. Formamide is known as reducing agent for silver nitrate in certain systems, too,⁴⁷ but we found that hydrazine was more suitable in our particular case.

When the silver nitrate inside the polymer capsules is reduced, the spherical shape of the nanocapsules is not changed compared to the empty polyurea capsules, as shown in Figure 13 by SEM measurements.

The nanocapsules containing a high amount of silver nanoparticles were found to have a bigger size: 328 nm for sample P47-Ag containing 6.8 wt % silver nitrate with respect to the dispersed phase and 208 nm for sample P38-Ag containing 1.2

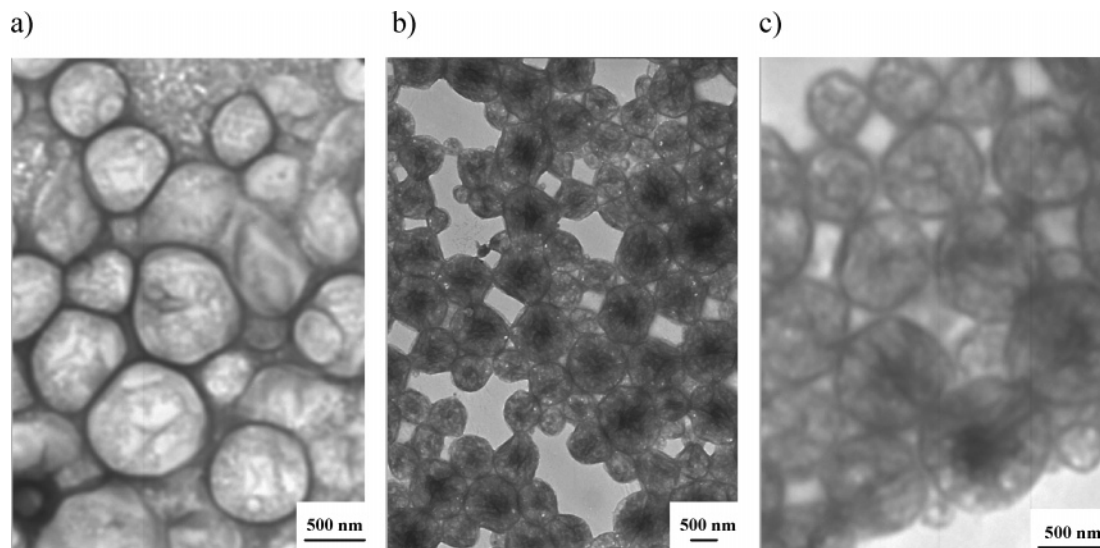


Figure 10. TEM micrographs of the nanocapsules: (a) sample P31, water as liquid core; (b, c) sample P24 (formamide as liquid core).

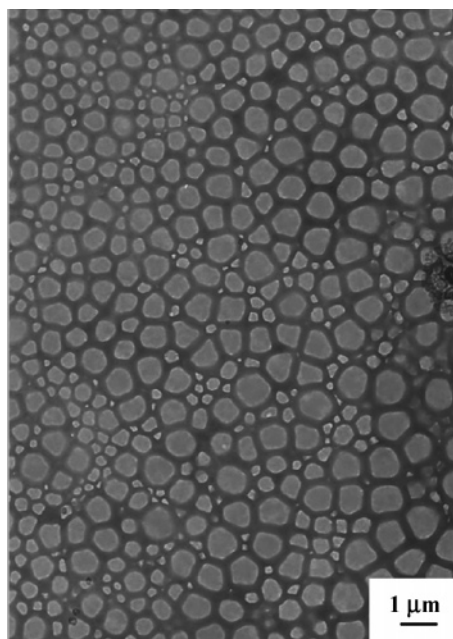


Figure 11. TEM micrograph of the polyurethane capsules from sample P20 of Table 2.

wt % silver nitrate. In fact, it is expected that the PEO part of the block copolymer surfactant probably binds the silver ions. Such an interaction lowers the efficiency of the surfactant. For the low amounts of silver nitrate in the nanocapsules, the silver nanoparticles average size increases from 24 to 29 nm when the size of the polymeric nanocontainers increases from 208 to 252 nm. For a high amount of silver nitrate (≥ 60 mg), the number of silver nanoparticles increases from 6 to 21 while the size of the nanocontainers increases from 239 to 328 nm (see Figure 14). In a general trend, the size of the capsules increases with the amount of silver nitrate. It has to be noted that no valid information about the size of the silver nanoparticles can be given by the DLS measurements. In principle, the silver nanoparticles may have a different coefficient of diffusion than the droplets surrounding them and a DLS program able to detect multimodal distribution of size could evidence this fact. But wide discrepancies in size observed between the DLS and the TEM measurements led to the conclusion that the DLS is not a suitable technique to measure the size of the silver nanoparticles in our particular case. This phenomenon could be explained by the fact that the synthesis of the silver nanoparticles was made without capping or stabilizing agent. The silver nanoparticles are probably stabilized by the polymeric wall of the capsules and hence reduce their mobility in the nanoreactors.

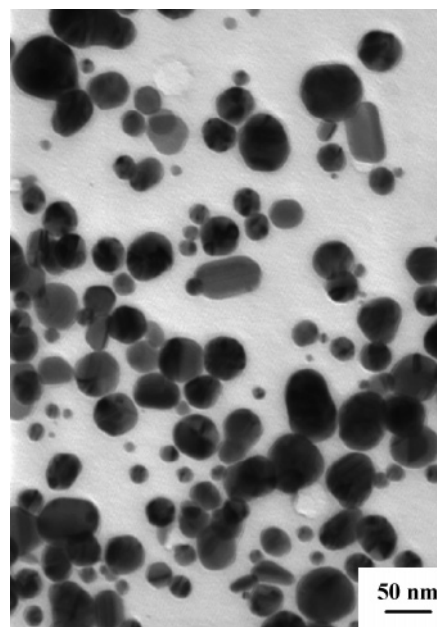


Figure 12. TEM micrograph of the control experiment: no second monomer was added to the miniemulsion.

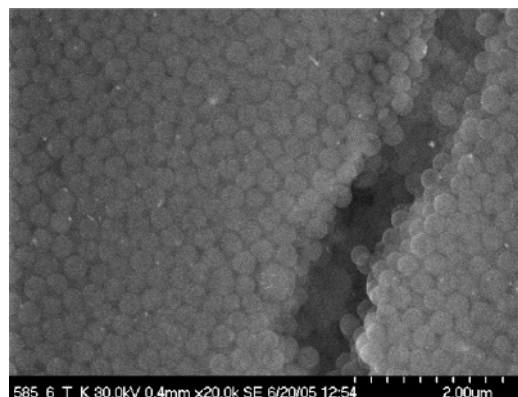


Figure 13. SEM micrographs of the capsules containing silver nanoparticles (sample P39-Ag).

The extinction UV-vis spectra shown in Figure 15 give also interesting information about the size, the shape, and the direct environment of the silver nanoparticles, which can be correlated to the TEM measurements, as shown in Figure 14. In general, very small silver nanoparticles (~ 2 nm) present the characteristics of a spectrum of a metallic crystal (and the plasmon band is damped due to the low electron density in the conduction band), whereas bigger nanoparticles show a (more intense) plasmon band. As shown in Table 6, the usual maximum absorbance λ_{\max} around 420 nm observed for spherical silver

Table 5. Characteristics of the Latexes Prepared with Different Amounts of Silver Nitrate

entry	AgNO ₃ (mg)	monomers		capsules diameter ^a (nm)	capsules diameter ^b (nm)	Ag NP diameter ^b (nm)	av no. of Ag NP per capsule ^b
		TDI (g)	DET (g)				
P38-Ag	20	0.25	0.1	221	208 ± 38	24 ± 2	1.08
P39-Ag	30	0.25	0.1	350	252 ± 47	29 ± 2	1.06
P40-Ag	30	0.25	0.1	378	277 ± 52	33 ± 2	1.33
P41-Ag	30	0.37	0.15	249	171 ± 32	27 ± 2	1.07
P42-Ag	30	0.37	0.15	268	185 ± 35	22 ± 1	1.39
P43-Ag	60	0.25	0.1	391	239 ± 45	14 ± 1	6.06
P44-Ag	60	0.25	0.1	272	266 ± 50	14 ± 1	3.4
P45-Ag	60	0.38	0.16	290	274 ± 51	26 ± 1	1.44
P46-Ag	60	0.39	0.16	293	271 ± 51	26 ± 2	3.78
P47-Ag	120	0.25	0.1	260	328 ± 61	16 ± 2	20.59

^a Determined by DLS. ^b Determined by TEM.

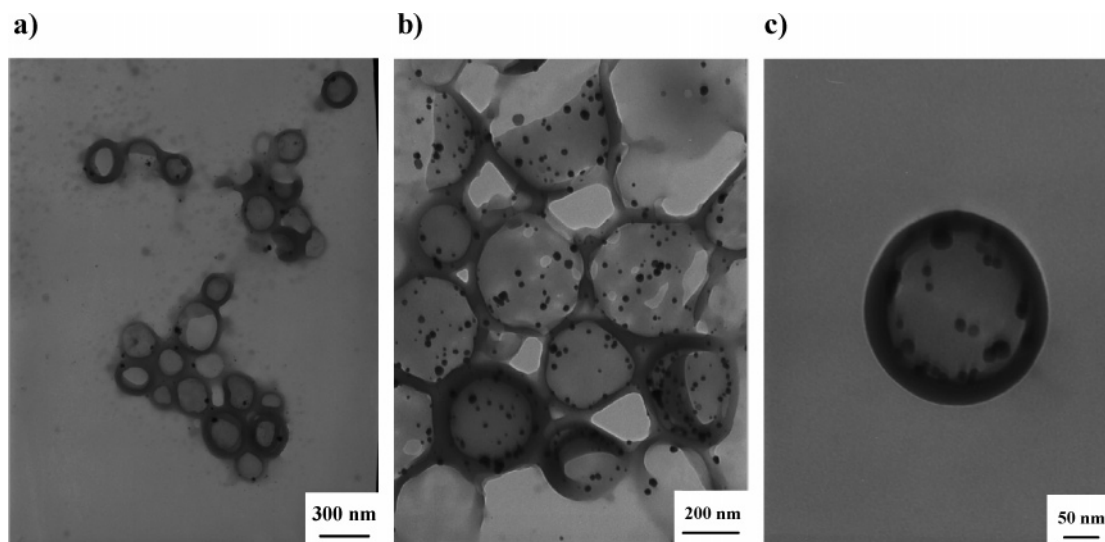


Figure 14. TEM micrographs of polyurea capsules loaded with different amounts of silver nanoparticles: (a) sample P39-Ag; (b, c) sample P47-Ag. It can be observed that sample P47-Ag contains much more silver nanoparticles than sample P39-Ag (see Table 5).

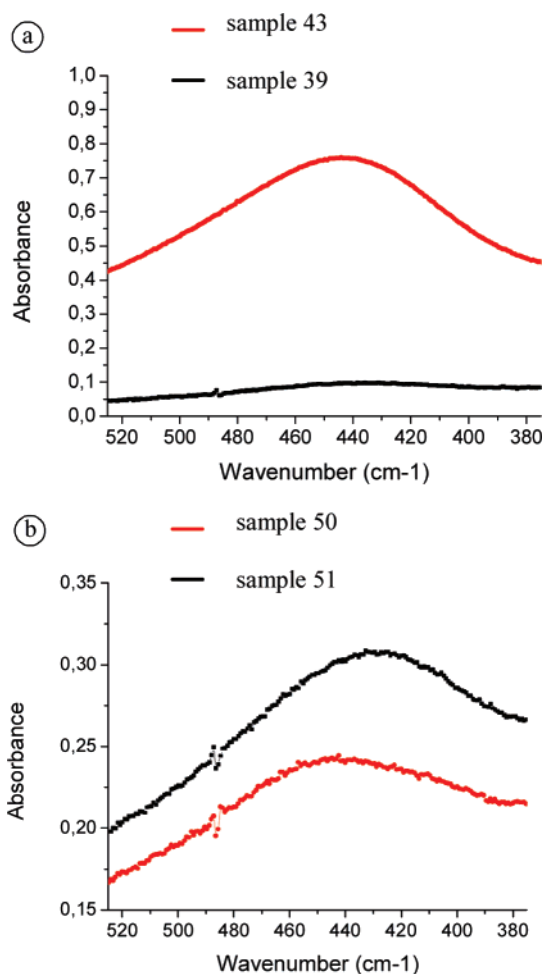


Figure 15. UV spectra of the silver/polyurea miniemulsions: (a) with formamide core; (b) with water core.

nanoparticles⁴⁸ is red-shifted when hydrazine is used as reducing agent independently of the nature of the hydrophilic solvent in the nanocapsules (water or formamide). It has to be noted that the polymeric capsules without silver nanoparticles inside do not contribute to the optical spectra in the 400–800 nm region. When the amount of silver nitrate increases, the plasmon band absorbance increases and λ_{\max} is red-shifted from $\lambda_{\max} = 431$ nm for entry P39-Ag ($[\text{AgNO}_3] = 0.14 \text{ g mol}^{-1}$) to $\lambda_{\max} = 444$

Table 6. Effect on the Silver Nitrate Concentration and the Reducing Agent on the Maximum of the Plasmon Band

entry	liquid core	AgNO_3^a (mol L^{-1})	reducing agent	λ_{\max} (nm)
P39-Ag	formamide	0.14	hydrazine	431
P48-Ag	formamide	0.14	formamide	419
P43-Ag	formamide	0.56	hydrazine	444
P49-Ag	formamide	0.56	formamide	400
P50-Ag	water	0.13	hydrazine	433
P51-Ag	water	0.25	hydrazine	442

^a Concentration in the dispersed phase; given in mol L^{-1} for the commodity of the reader in order to compare with data from other publication. For conversion see Table 5.

nm for entry P43-Ag ($[\text{AgNO}_3] = 0.56 \text{ g mol}^{-1}$) with a formamide core and from $\lambda_{\max} = 433$ nm for entry P50-Ag ($[\text{AgNO}_3] = 0.13 \text{ g mol}^{-1}$) to $\lambda_{\max} = 442$ nm for entry P51-Ag ($[\text{AgNO}_3] = 0.25 \text{ g mol}^{-1}$) with an aqueous core. When formamide is used as a reducing agent and the hydrophilic agent, then λ_{\max} decreases as the concentration of the silver nitrate increases (P48-Ag and P49-Ag).

Contrary to the work of Sarkar et al.,⁴⁷ we made bigger silver nanoparticles, hence yielding a red shift of the plasmon band, when the concentration of silver nitrate increases, as shown in Table 5. The size of the nanoparticles depends mainly on the nucleation and growth processes, either the growth by autocatalysis or the growth by ripening. We believe that the “film” or surrounding layer around the silver during the synthesis is very flexible since we did not add any compounds such as protective colloids to stabilize them. In this case, the growth is controlled by the ripening according to Tojo et al.⁴⁹ Thus, an increase of the silver nitrate concentration leads to both more nanoparticles and bigger ones, when the fast reduction process by hydrazine is used. In the case of using formamide as reduction agent, the reduction process is much slower.

Double-Shell Capsules. Particles and capsules can be synthesized via the condensation between a monomer present in the dispersed phase and a monomer present in the continuous phase. As discussed above, it is possible to increase the wall thickness of the nanocapsules by increasing the amount of monomers employed. We wanted to test another approach to increase the shell thickness of the capsules and to form capsules with two different polymeric shells. Thus, we increased the wall thickness of the previously synthesized polyurea nanocapsules by coating the nanocapsules via free-radical polymerization of

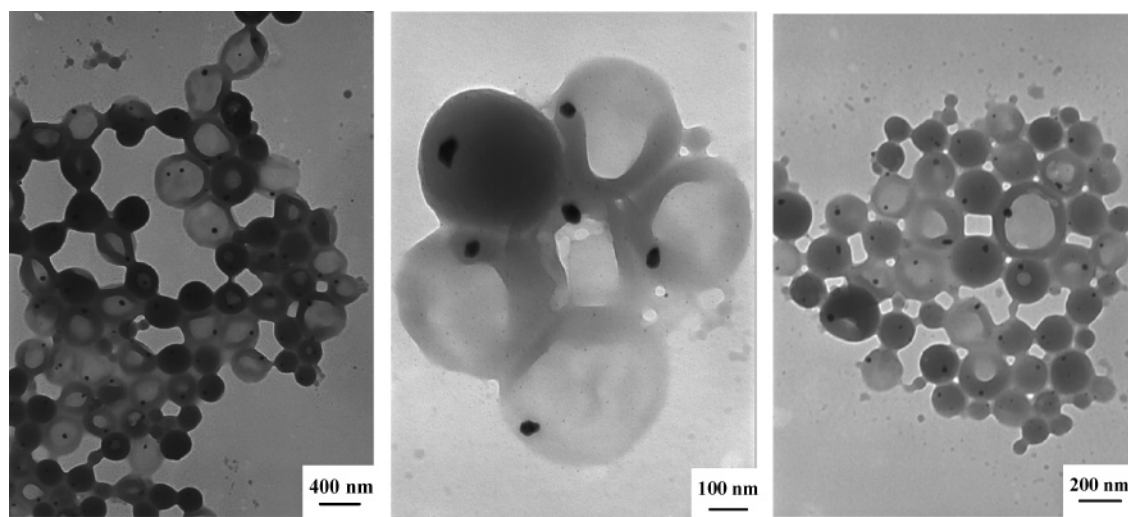


Figure 16. TEM micrographs of the polyurea nanocapsules coated with poly(vinylcaprolactam) (sample P52).

Table 7. Characteristics of the Latex P52 before and after Coating with Poly(vinylcaprolactam)

characteristics	before coating	after coating
nanocapsule diameter ^a (nm)	280	330
silver nanoparticles diameter ^a (nm)	18	

^a Determined by TEM.

a third monomer around the shell. *N*-Vinylcaprolactam was polymerized around polyurea nanocapsules containing silver nanoparticles prepared with the standard recipe, as shown in Figure 16. We chose this monomer because the monomer is hydrophobic but gives an amphiphilic polymer, which should stay at the interface of the nanocapsules. Thus, we obtained a rather complex material in a one-pot synthesis with three different steps: interfacial polycondensation to form the polyurea shell, reduction of the encapsulated silver salt to produce the silver nanoparticles, and finally free-radical polymerization to generate a second shell (see Table 7).

Conclusion

Hollow polymeric capsules containing a hydrophilic liquid core were obtained in a simple one-pot miniemulsion process without the use of a sacrificial core. The polyurea, polythiourea, or polyurethane shells are made by polycondensation at the interface of the droplets. The functionality of the shell is governed by the nature of the monomers and the ratio between the two monomers introduced in the miniemulsion. The size of the capsule is dependent not only on the concentration of the surfactant but also on the time of addition of the second monomer. The thickness of the wall of the capsules is controlled by the amount of monomers employed. The shape of the capsules was always found to be spherical except when diethylenetriamine in water was used as the dispersed phase. Capsules loaded with silver nanoparticles were synthesized upon reduction of silver nitrate encapsulated in polyurea shell.

It is possible to increase the wall thickness of the nanocapsules by increasing the amount of monomers. In another approach we increased the wall thickness by coating the nanocapsules by polymerizing a third monomer around the shell. *N*-Vinylcaprolactam was polymerized around polyurea nanocapsules containing silver nanoparticles prepared with the standard recipe. We chose this monomer because it is hydrophobic but gives an amphiphilic polymer, which stays at the interface of the nanocapsules. Thus, we obtained a rather complex material in

a one-pot synthesis with three different steps: interfacial polycondensation to make the polyurea shell, reduction of the encapsulated silver salt to make the silver nanoparticles, and finally free-radical polymerization to make a second shell.

Remarkably, the capsules were found to be redispersible in water. The polyurea is also a biocompatible material, which makes these capsules suitable for biomedical application. For instance, polyurea microcapsules synthesized with diethylene triamine and tolylene 2,4-diisocyanate were found to have excellent oxygen-binding abilities in their use as artificial red blood cells.⁵⁰ Thus, it would be interesting in the future to study the membrane permeability and the efficiency of these capsules as drug-delivery systems.

Acknowledgment. The authors thank H. Schlaad for the synthesis of the poly[(butylene-*co*-ethylene)-*b*-(ethylene oxide)], P(B/E-*b*-EO), copolymer. We gratefully acknowledge Marlies Fritz for the DSC and TGA measurements, Elvira Kaltenecker for the IR measurements, Achim Manzke for helpful discussions, and Dr. Axel Schaz for the SLS measurements.

References and Notes

- (1) Caruso, F. *Adv. Mater.* **2001**, *13*, 11–22.
- (2) Caruso, F.; Caruso, R. A.; Mohwald, H. *Science* **1998**, *282*, 1111–1114.
- (3) Caruso, F.; Caruso, R. A.; Mohwald, H. *Chem. Mater.* **1999**, *11*, 3309–3314.
- (4) Caruso, F.; Spasova, M.; Salgueirino-Maceira, V.; Liz-marzan, L. M. *Adv. Mater.* **2001**, *13*, 1090–1094.
- (5) Park, M.; Xia, C.; Advincula, R. C.; Schutz, P.; Caruso, F. *Langmuir* **2001**, *17*, 7670–7674.
- (6) Duan, H.; Chen, D.; Jiang, M.; Gan, W.; Li, S.; Wang, M.; Gong, J. *J. Am. Chem. Soc.* **2001**, *123*, 12097–12098.
- (7) Fleming, M. S.; Mandal, T. K.; Walt, D. R. *Chem. Mater.* **2001**, *13*, 2210–2216.
- (8) Bourgeat-Lami, E.; Lang, J. J. *Colloid Interface Sci.* **1998**, *197*, 293–308.
- (9) Bourgeat-Lami, E.; Lang, J. J. *Colloid Interface Sci.* **1999**, *210*, 281–289.
- (10) Zhang, K.; Chen, H.; Chen, X.; Chen, Z.; Chen, Z.; Cui, Z.; Yang, B. *Macromol. Mater. Eng.* **2003**, *288*, 380–385.
- (11) Zha, L.; Zhang, Y.; Yang, W.; Fu, S. *Adv. Mater.* **2002**, *14*, 1090–1092.
- (12) Xu, X.; Asher, S. A. *J. Am. Chem. Soc.* **2004**, *126*, 7940–7945.
- (13) Perruchot, C.; Khan, M. A.; Kamitsi, A.; Armes, S. P.; von Werne, T.; Patten, T. E. *Langmuir* **2001**, *17*, 4479–4481.
- (14) von Werne, T.; Patten, T. E. *J. Am. Chem. Soc.* **2001**, *123*, 7497–7505.
- (15) Mori, H.; Seng, D. C.; Zhang, M.; Muller, A. H. *Langmuir* **2002**, *18*, 3682–3693.

- (16) Kamata, K.; Lu, Y.; Xia, Y. *J. Am. Chem. Soc.* **2003**, *125*, 2384–2385.
- (17) Mandal, T. K.; Fleming, M. S.; Walt, D. R. *Chem. Mater.* **2000**, *12*, 3481–3487.
- (18) Zhou, Q. Y.; Wang, S. X.; Fan, X. W.; Advincula, R. C. *Langmuir* **2002**, *18*, 3324–3331.
- (19) Marinakos, S. M.; Novak, J. P.; Brousseau, L. C., III.; House, A. B.; Edeki, E. M.; Feldhaus, J. C.; Feldheim, D. L. *J. Am. Chem. Soc.* **1999**, *121*, 8518–8522.
- (20) Jiang, P.; Bertone, J. F.; Colvin, V. L. *Science* **2001**, *291*, 453–457.
- (21) Ganachaud, F.; Katz, J. L. *ChemPhysChem* **2005**, *6*, 209.
- (22) Wong, M. S.; Cha, J. N.; Choi, K.; Deming, T. J.; Stucky, D. *Nano Lett.* **2002**, *2*, 583–587.
- (23) Lestage, D. J.; Urban, M. *Langmuir* **2005**, *21*, 4266–4267.
- (24) Liu, S.; O'Brien, D. F. *J. Am. Chem. Soc.* **2002**, *124*, 6037–6042.
- (25) Pavlyuchenko, V. N.; Sorochinskaya, O. V.; Irvanche, S. S.; Klubin, V. V.; Kreichman, G. S.; Budto, V. P.; Skrifvars, M.; Halme, E.; Koskinen, J. *J. Polym. Sci., Part A: Polym. Chem.* **2001**, *39*, 1435–1449.
- (26) Okubo, M.; Konishi, Y.; Minami, H. *Colloid Polym. Sci.* **1998**, *276*, 638–642.
- (27) McDonald, C. J.; Bouck, K. J.; Chaput, A. B.; Stevens, C. J. *Macromolecules* **2000**, *33*, 1593–1605.
- (28) Minami, H.; Kobayashi, H.; Okubo, M. *Langmuir* **2005**, *21*, 5655–5658.
- (29) Minami, H.; Okubo, M.; Oshima, Y. *Polymer* **2005**, *46*, 1051–1056.
- (30) Ley, S. V.; Ramarao, C.; Lee, A. L.; Ostergaard, N.; Smith, S. C.; Shirley, I. M. *Org. Lett.* **2003**, *5*, 185–187.
- (31) Pears, D. A.; Smith, S. C. *Aldrichim. Acta* **2005**, *38*, 23–33.
- (32) Paiphansiri, U.; Tangboriboonrat, P.; Landfester, K. *Macromol. Biosci.* **2006**, *6*, 33–40.
- (33) Tiarks, F.; Landfester, K.; Antonietti, M. *Langmuir* **2001**, *17*, 908–918.
- (34) Rajot, I.; Bone, S.; Graillat, C.; Hamaide, Th. *Macromolecules* **2003**, *36*, 7484–7490.
- (35) Luo, Y.; Zhou, X. *J. Polym. Sci., Part A: Polym. Chem.* **2004**, *42*, 2145–2154.
- (36) Torini, L.; Argillier, J. F.; Zydowicz, N. *Macromolecules* **2005**, *38*, 3225–3236.
- (37) Scott, C.; Wu, D.; Ho, C.-C.; Co, C. C. *J. Am. Chem. Soc.* **2005**, *127*, 4160–4161.
- (38) Breitenkamp, K.; Emrick, T. *J. Am. Chem. Soc.* **2003**, *125*, 12070–12071.
- (39) Im, S. H.; Jeong, U.; Xia, Y. *Nat. Mater.* **2005**, *4*, 671–675.
- (40) Taira, S.; Du, Y.-Z.; Kodaka, M. *Biotechnol. Bioeng.* **2006**, *93*, 396–400.
- (41) Schlaad, H.; Kukula, H.; Rudloff, J.; Below, I. *Macromolecules* **2001**, *34*, 4302–4304.
- (42) Montenegro, R.; Antonietti, M.; Landfester, K. *J. Phys. Chem. B* **2003**, *107*, 5088–5094.
- (43) Takasu, M.; Kawaguchi, H. *Colloid Polym. Sci.* **2005**, *283*, 805–811.
- (44) Landfester, K. *Macromol. Rapid Commun.* **2001**, *22*, 896–936.
- (45) Crespy, D.; Landfester, K. *Macromolecules* **2005**, *38*, 6882–6887.
- (46) Yang, M.; Wang, W.; Yuan, F.; Zhang, X.; Liang, F.; He, B.; Minch, B.; Wegner, G. *J. Am. Chem. Soc.* **2005**, *127*, 15107–15111.
- (47) Sarkar, A.; Kapoor, S.; Mukherjee, T. *J. Phys. Chem. B* **2005**, *109*, 7698–7704.
- (48) Mock, J. J.; Barbic, M.; Smith, D. R.; Schultz, D. A.; Schultz, S. *J. Chem. Phys.* **2002**, *116*, 6755–6759.
- (49) Tojo, C.; Blanco, M. C.; Rivadulla, F.; Lopez-Quintela, M. A. *Langmuir* **1997**, *13*, 1970–1977.
- (50) El-Gibaly, I.; Anwar, M. *Int. J. Pharm.* **2004**, *278*, 25–40.

MA0621932